

Electronic Supplementary Information (ESI) for the article entitled:

Remarkably enhanced Red-NIR broad spectral absorption via gold nanoparticles: applications for organic photosensitive diodes

Xiao Luo^a, Lili Du^a, Zhanwei Wen^a, Wenli Lv^a, Feiyu Zhao^a, Xinyu Jiang^a, Yingquan Peng^{a, b, *}, Lei Sun^a, Yao Li^a, and JinWei Rao^b

^a *Institute of Microelectronics, School of Physical Science and Technology, Lanzhou University, South Tianshui Road 222#, Lanzhou 730000, China*

^b *Key Laboratory for Magnetism and Magnetic Materials of the Ministry of Education, Lanzhou University, South Tianshui Road 222#, Lanzhou 730000, China*

The X-ray diffraction (XRD) spectra analysis: waterfall plots of XRD measurements of the quartz/NPB/AuNPs/C₆₀/BCP film structure with different gold nano-island thickness were shown in **Figure S1** by using a D/max-2400 (Rigaku, Japan) with Cu K α radiation. All films showed broad diffraction peaks at 2 θ values of about 20°, corresponding to the (220) and (311) crystalline planes of C₆₀.¹ It is worth to note that the intensity for the broad diffraction peaks of C₆₀ became decreased as the increase of the thickness of the added AuNPs from 3 nm to 6 nm, indicating that the crystallinity of subsequent grown C₆₀ began to weaken. On the other hand, there was no crystallization peak of gold when 1-nm AuNPs were added in the interface of NPB/C₆₀ heterojunction. However, an obvious peak appeared at 38.3°, which were assigned to diffraction from the {111}. Moreover, other peaks appeared at about 44.5°,

* Corresponding author at: Institute of Microelectronics, School of Physical Science and Technology, Lanzhou University, South Tianshui Road 222#, Lanzhou 730000, China.

E-mail address: yqpeng@lzu.edu.cn (Y. Peng).

64.7°, 77.8° and 81.8°, respectively, as increased thickness of AuNPs. These observations confirmed that vacuum-thermal-deposited AuNPs were nanocrystalline in nature and nanoplates were mainly dominated by {111} facets.²

Photosensitive characteristics of OPDs: Figure S2 showed the R , EQE and D^* values of the OPDs as a function of the light power. It can also be observed from Figure S2 that the spectrum responsivity (R), external quantum efficiency (EQE) and the detectivity (D^*) depends almost linearly on the incident optical power at the log-log coordinate. In addition, the three critical parameters above decreased gradually as the illumination power increased, indicating that the highest photoelectric parameter was obtained in lower optical power. Note that the plasmonic OPDs (red line) exhibited better characteristics than the control device (black line) no matter at either 0V or -0.4V. On the whole, an order of magnitude improvement of photosensitive performance was achieved by plasmon resonance absorption of AuNPs with regard to the above-mentioned parameters. In future, a more size-controllable formation of AuNPs or Au cluster may lead to a well-defined size distribution, which could be used to optimize the absorption of the particles for adjusting absorption spectrum and improving optical detection performance.

FDTD Simulation and plasmonic electric field distribution: Electromagnetic field distributions of the AuNP were simulated by the three-dimensional FDTD method³ with the commercial package CST STUDIO SUITE™. Based on TEM images, the shape of AuNP built in the simulation program was simplified as a sphere with 3-nm diameter. The exciting light source was a linearly polarized plane wave of 650 nm and 830 nm wavelength, respectively. Some more visible details about the simulation model were displayed in Figure S3.

Figure S4 showed a comparison of the near electric field distribution for the X-, Y-, Z- and absolute-component under light excitation with a wavelength of 650 nm, and the electric phase was fixed at 0 degrees. It could be found that the X-component had the largest electric field distribution (Figure S4a) with respect to Y and Z-component,

almost similar to the absolute-component. Besides, Z-component was the smallest for the near electric field distribution. Therefore, the X-component could be viewed as the dominant component of the electric field distribution. That is to say, the near field induced by AuNPs was mainly distributed in the X-orientation when the exciting light was perpendicularly incident from the Z-direction. Correspondingly, the comparison of the near electric field distribution for the X-, Y-, Z- and absolute-component under 830 nm light excitation was not shown here, similar to those under 650 nm case.

Furthermore, **Figure S5** showed a comparison of the near electric field distribution for different electric phase (0° , 45° , 90° , 135° and 180°) under 650 nm and 830 nm light excitation. It is noteworthy that different electric phase showed different plasmonic electric field distribution. The electric field intensity was the smallest when the electric phase is 90 degrees.

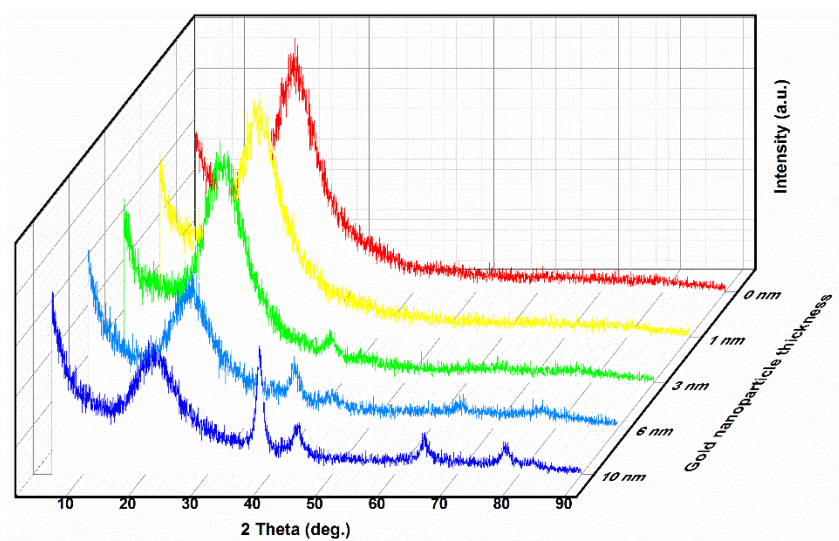


Figure S1. Waterfall plots of XRD measurements for the quartz/NPB/AuNPs/C₆₀/BCP with different gold nano-island thickness.

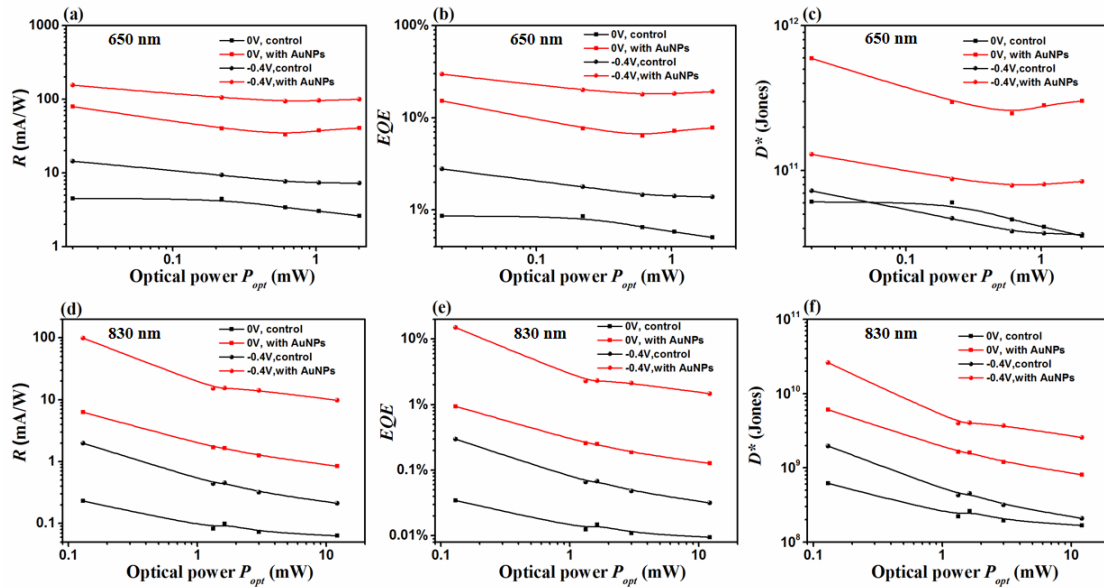


Figure S2. The dependence of responsivity R ((a), (d)), external quantum efficiency EQE ((b), (e)) and specific detectivity D^* ((c), (f)) on optical power P_{opt} for different OPDs (reference and plasmonic device) under different illumination wavelengths (650 nm and 830 nm) different applied voltages (0V and -0.4V). (a)-(c) is corresponding to 650 nm illumination, and (d)-(f) is corresponding to 830 nm illumination.

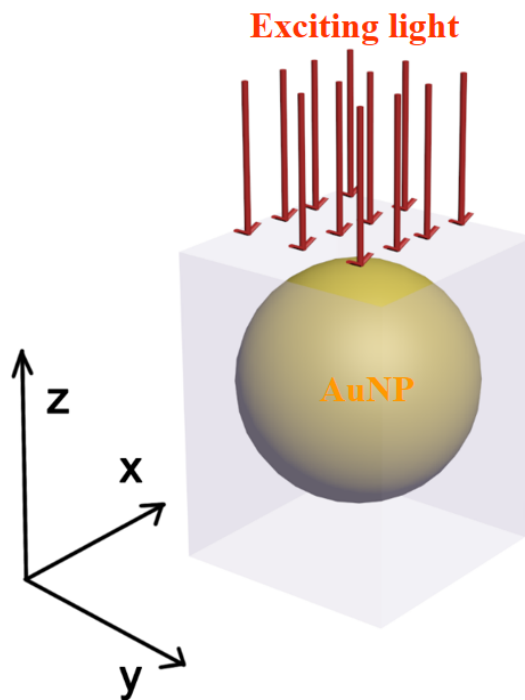


Figure S3. The schematic diagram of 3D model for FDTD simulation of AuNP

excited by laser illumination.

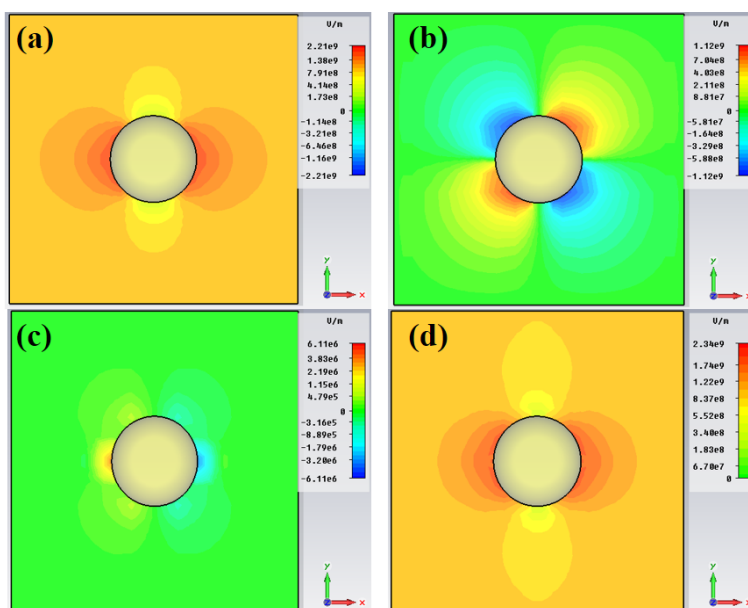


Figure S4. The plasmonic electric field distribution of the 3 nm AuNPs, calculated at a wavelength of 650 nm using a 3D FDTD method when the electric phase is 0 degrees. (a) The X-component; (b) the Y-component; (c) the Z-component; (d) the absolute component.

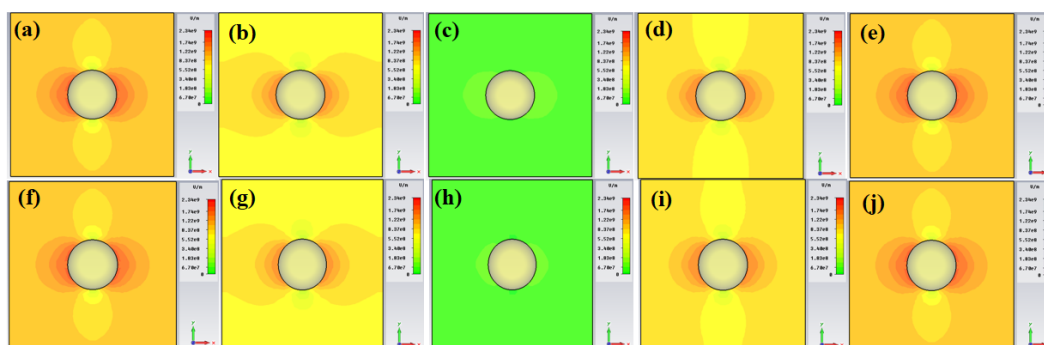


Figure S5. The plasmonic electric field distribution of the 3 nm AuNPs, calculated by using a 3D FDTD method. (a)-(e) were excited under the 650 nm laser, corresponding to the electric phase 0° , 45° , 90° , 135° and 180° , respectively. (f)-(j) were excited under the 830 nm laser, corresponding to the electric phase 0° , 45° , 90° , 135° and 180° , respectively.

References:

- (1) A. F. Hebard, R. C. Haddon, R. M. Fleming, A. R. Kortan, *Applied Physics Letters*, 1991, **59**, 2109.
- (2) Y. Shao, Y. Jin, S. Dong, *Chem. Commun.* 2004, **9**, 1104-1105.
- (3) C. Oubre, P. Nordlander, *The Journal of Physical Chemistry B*, 2004, **108**, 17740-17747.